Baba Ismail YM, Wimpenny I, Bretcanu O, Dalgarno K, El Haj AJ.

Development of multi-substituted hydroxyapatite nanopowders as biomedical materials for bone tissue engineering applications.

***Journal of Biomedical Materials Research Part A* 2017**

DOI: http://dx.doi.org/10.1002/jbm.a.36038

Development of multi-substituted hydroxyapatite nanopowders as biomedical materials for bone tissue engineering applications

Yanny M Baba Ismail[1,2, 3], Ian Wimpenny[4], Oana Bretcanu[2], Kenneth Dalgarno[2], Alicia J El Haj[1]

[1]Institute for Science and Technology in Medicine, Keele University Medical School, Stoke-on-Trent, ST47QB, United Kingdom.

[2]School of Mechanical and Systems Engineering, Newcastle University, NE17RU, United Kingdom.

[3]School of Materials and Mineral Resources Engineering, Universiti Sains Malaysia, Engineering Campus, 14300, Nibong Tebal, Penang, Malaysia.

[4]Institute of Population Health, University of Manchester, Manchester, M139PL, United Kingdom.

Corresponding author: yannymarliana@usm.my; +604-5996154 (tel); +604-5991011 (fax)

ABSTRACT

Ionic substitutions have been proposed as a tool to control the functional behavior of synthetic hydroxyapatite (HA), particularly for Bone Tissue Engineering (BTE) applications. The effect of simultaneous substitution of different levels of carbonate (CO_3) and silicon (Si) ions in the HA lattice was investigated. Furthermore, human bone marrow-derived mesenchymal stem cells (hMSCs) were cultured on multi-substituted HA (SiCHA) to determine if biomimetic chemical compositions were osteoconductive. Of the four different compositions investigates, SiCHA-1 (0.58wt% Si) and SiCHA-2 (0.45wt% Si) showed missing bands for CO_3 and Si using FTIR analysis, indicating competition for occupation of the phosphate site in the HA lattice. 500°C was considered the most favourable calcination temperature as: (i) the powders produced possessed a similar amount of CO_3 (2-8wt%) and Si (<1.0wt%) as present in native bone; and (ii) there was a minimal loss of CO_3 and Si from the HA structure to the surroundings during calcination. Higher Si content in SiCHA-1 led to lower cell viability and at most hindered proliferation, but no toxicity effect occurred. While, lower Si content in SiCHA-2 showed the highest ALP/DNA ratio after 21 days culture with hMSCs, indicating that the powder may stimulate osteogenic behaviour to a greater extent than other powders.

Key Words: hydroxyapatite, carbonate, silicon, *in vitro* test, human mesenchymal stem cells

INTRODUCTION

In the 1980's, Hydroxyapatite (HA) was considered to be the material of choice for the development of bone substitutes to repair bone fractures and other defects due to its strong affinity with the mineral constituents of bones, good bioactivity, osteoconductivity and biocompatibility with the human bone tissue [1-5]. Although, stoichiometric HA, composed of calcium (Ca), phosphates (PO_4) and hydroxyl (OH) groups [Ca_{10} $(PO_4)_6$ $(OH)_2$], the chemical composition of biological apatites differs from the stoichiometric HA [6-9]. The biological apatites are uniquely similar in that they all comprise carbonate (CO_3) in varying amounts of 2-8wt%, preferentially substituting the phosphate site (B-type) compared with hydroxyl (A-type) ions in the apatite lattice [9-13]. The composition of CO_3 depends on bone age, site, sex and health of the individual [8, 14, 15].

The beneficial impact of CO_3 substitution into phosphate and/or hydroxyl site in HA structure has been reported in the literature. For instance, the presence of B-type CO_3-HA (CHA) has been shown to cause a decrease in crystallinity and enhance solubility both *in vitro* and *in vivo* [6, 16, 17]. *In vivo* tests using an ovine model demonstrated that more dissolution was observed from the CHA at the bone implant interface and within the implant, when compared to pure HA [18].

Among other trace elements present in natural bone, silicon (Si) plays an important role in early stage of bone formation [5, 19]. Back in 1970's, Carlisle found that Si deficiency resulted in abnormal bone formation and this finding was supported by Schwartz & Milne who confirmed that Si play an important role as cross-linking agent in connective tissue and its importance to vascular health [20, 21]. Si also plays an important role in bone metabolism [20, 22]. At physiological levels, soluble Si was reported to enhance osteoblastic cell proliferation and differentiation [23], stimulates

the enzymes involved in collagen type I synthesis [19] and increases the bone mineral density (BMD) [24]. However, there is still a discrepancy on the effect of Si-substituted HA (SiHA) on biological responses, which has been reported in the literature. This is mainly because Si substitution into HA lattice is known to have a dose-dependent effect on the proliferation, differentiation and collagen synthesis of osteoblast, with a direct influence on the remodelling process and osteoclast development and resorption activities [8, 24-26].

In this context, we are now focussing on the development of silicon-carbonated HA (SiCHA) powders with a fully controlled level of CO_3- and Si-substitutions into the HA structure as this may result in synergy between the bioresorbable properties of CHA and the release of soluble Si [15, 26]. To date, several studies on the development of SiCHA powders focused on different synthesis techniques, physico-chemical characterizations and some solubility tests in simulated body fluid (SBF) to predict the ability to form apatite layer *in vitro* [6, 7, 27-29]. However, to our knowledge, limited investigations have considered the cell responses. Recently, Landi and colleagues have highlighted the benefits of CHA, SiHA and SiCHA in stimulating better cell responses compared to HA alone, where high Si content (0.88wt%) substituted the HA lattice was found to cause a toxic effect to human osteoblasts cells [8]. Even though these bioceramics are easily producible by both dry and wet chemical method and appear to be biocompatible in their bulk form, knowledge concerning the effect of ionic substitutions into the HA structure and their releases to the surrounding cells during culture are still lacking. Therefore, the aim of the present study was to develop SiCHA powders with controlled amounts of CO_3- and Si-substituted into the apatite structure to closely mimic the range of compositions observed within bone mineral and investigated the effect of ionic

substitutions in response to human bone marrow derived-mesenchymal stem cells to finally select the most osteoconductive powders as the potential biomedical materials for BTE applications.

MATERIALS AND METHODS

Preparation of powders

The synthesis of silicon-carbonated HA (SiCHA) powders was performed based on a nanoemulsion method at ambient temperature described elsewhere [27]. Acetone was used as organic solvent to create the nanoemulsion phase. An acetone solution of calcium nitrate tetrahydrate, $Ca(NO_3)_2.4H_2O$ (99.0% pure) was added dropwise into the di-ammonium hydrogen phosphate, $(NH_4)_2HPO_4$ (98.0% pure), ammonium hydrogen carbonate, NH_4HCO_3 (99.0% pure) and silicon tetra acetate, $Si(CH_3COO)_4$ (98.0% pure) in aqueous solution; all reactants were purchased from Sigma-Aldrich. Four different groups of powders with different CO_3 *(x)* and Si *(y)* molar contents were synthesized in this work: CO_3-substituted HA (CHA), Si-substituted HA (SiHA) and silicon-carbonated HA (SiCHA-1 and SiCHA-2), as shown in Table 1. The general formula for the synthesized powders can be written as follows:

CHA $Ca_{10-x/2}(PO_4)_{6-x}(CO_3)_x(OH)_2$ (1)

SiHA $Ca_{10}(PO_4)_{6-y}(SiO_4)_y(OH)_{2-y}$ (2)

SiCHA $Ca_{10-x/2}(PO_4)_{6-x-y}(CO_3)_x(SiO_4)_y(OH)_{2-y}$ (3)

Prior to production of SiCHA powders, pure CHA and SiHA were synthesized to optimize the composition of CO_3- and Si- substituted into the apatite structure. The compositions of the pure CHA (x= 2.0) and SiHA (y= 0.3 and 0.5) powders were

chosen to closely mimic the composition of CO_3- and Si in bone mineral; these powders then used as the control compositions.

Calcination was then performed on the as-synthesized powders at 500, 600 and 700°C with a heating rate of 10°C /min and at least one hour soaking time in ambient atmosphere.

Physical and chemical characterization techniques

Physical and chemical characterizations were firstly performed to optimize the calcination temperatures. Powders having the closest compositions to the natural human bone mineral were selected as the optimum condition.

X-Ray Diffraction Analysis

X-Ray Diffraction (XRD) was used to determine the crystallinity of powders after calcination. XRD was carried out using a Bruker D8 XRD with a copper anode (Cu K_α, λ=1.5406 Å) as X-Ray source. The range of x-ray scan was fixed from 2θ=10° to 90°. HA standard pattern with ICDD file number of 09-0432 was used as the reference pattern. Data analyses were done using X'Pert HighScore Plus software. Lattice parameters and crystallite size were calculated based on Rietveld refinement.

Fourier Transform Infra-Red Spectroscopy

Fourier Transform Infra-Red (FTIR) Spectroscopy was used to identify any changes in the mechanisms of CO_3 and Si ions substitution within the HA structure after calcination. The wavenumber range was 4000 to 650 cm^{-1}; with a spectral resolution of Spectrum 100 Software. Each sample was scanned four times using transmittance mode.

Transmission Electron Microscopy

Philips CM100 Transmission Electron Microscope (TEM) was used to examine the morphology of the calcined powders in terms of their particle size and shape. Prior imaging the samples, 0.1 mg of powders were suspended in pure water and sonicated for ten minutes to allow the powders to be well dispersed. A drop of the suspension was then carefully placed onto a copper grid (diameter=3.05 μm, mesh=400) and allowed to dry. Samples were imaged at a magnification of 130 kX at HV=100.0kV.

Carbon, Hydrogen, Nitrogen Analysis

The percentages of CO_3 incorporated in the calcined powders were determined using Carbon, Hydrogen, Nitrogen (CHN) analysis using Carlo Erba 1180 Elemental Analyser controlled with CE Eager 200 Software, run in accordance to the manufacturer's instruction and weighed using a certified Mettler MX5 Microbalance. The powders (1.5-2.0 mg) were combusted at high temperatures in a stream of oxygen, and the products of the combustion for carbon, hydrogen and nitrogen were measured by the instrument in a single analysis. In order to estimate the amount of CO_3 present in the sample, the wt% of carbon obtain was multiplied by a factor of five [10, 32].

Inductively Coupled Plasma-Optical Emission Spectroscopy Measurement

0.01 g of the calcined powders was digested in 1 M HNO_3 (2.5 mL of HNO_3, 1.5 mL of H_2O_2, and 0.3 mL of HCl) in a 100 mL Erlenmeyer flask. The concentrations of Ca, P and Si in the calcined powders were determined by

inductively coupled plasma with optical emission spectroscopy (ICP-OES) using Perkin Elmer Optimal 4300DV instrument.

X-Ray Fluorescence Analysis

X-Ray Fluorescence (XRF) is an emission spectroscopic technique, which identify the elements present in the sample. The ratio of Ca/P and percentages of Si that successfully incorporated into the apatite structure were determined using XRF. The sample preparation and analysis of the calcined powders were performed at Glass Technology Service (GTS) in Sheffield. The elemental compositions in the powders were quantified using a Rigaku RIX-3000 wavelength dispersive XRF spectrometer. The 2910a sample (54.48% CaO, 41.25% P_2O_5, 0.21% SiO_2, 0.043% Na, 0.011% Mg, 0.094% Al, 0.078% Sr, 0.011% Fe and 0.01% Zr) was used as check standards for the analysis, which were run pre- and post-sample analyses to ensure the accuracy of the results obtained.

***In vitro* biocompatibility assessment**

International Organization for Standardization (ISO) 10993-5: Biological Evaluation of Medical Devices, Part 5: Tests for Cytotoxicity, was adapted and used as guideline in this study. This test involved the study on the cell viability, proliferation, metabolic activity and early osteogenic differentiation of hMSCs in direct contact with the investigated samples. The *in vitro* biocompatibility test was performed only on the optimized calcined powders.

Sample Preparation

As all samples tested were in powder form, aliquots of 0.05 g of the optimized calcined powders were sterilized in 1.0 mL of 70% industrial methylated spirit (IMS) for three hours followed by rinsing twice with PBS.

Cell culture and seeding

Human bone marrow derived-mesenchymal stem cells (hMSCs) obtained from a 24-year old male (Lonza, United States) at passage zero (P0) were expanded until passage two (P2) when the required cell number was obtained. Cells were cultured in high glucose expansion media consists of 4.5g/L Dulbecco's Modified Eagle Medium, DMEM (Lonza, United Kingdom), 1% v/v L-glutamine (Lonza, United Kingdom), 1% v/v Penicilin-Streptomycin (Lonza, United Kingdom) and 10% v/v Fetal Bovine Serum (Biosera labtech, United Kingdom) followed by, incubation at humidified environment at 37°C with 5% CO_2. hMSCs at passage 3 (P3) were seeded at $5X10^4$ per well in a 24 well cell culture plate and allowed to adhere for three hours. Prior to direct contact of the powders with the seeded cells, 1.0 mL of osteogenic media was directly added into the aliquots containing 0.05 g of sterile powders, mixed well and carefully transferred to the relevant wells. Culture media was replenished every three days for 21 days. A glass pipette was used to carefully discard the media from the side of the relevant wells without disrupting the culture. In all cases, tissue culture plastic alone cultured in osteogenic media acts as the positive control (non-toxic) whilst negative control (toxic) consists of 0.1% Triton-X in high glucose expansion media. At 7, 14 and 21 days, cells were rinsed with Phosphate Buffer Saline, PBS (Sigma-Aldrich, United Kingdom), trypsinized, washed again

with PBS and samples were lysed in 1.0 mL of dH_2O followed by being frozen at -80°C.

Cell viability

The cell viability was observed using Confocal Laser Scanning Microscope (CLSM) Olympus Fluoview FV 1200 with Fluoview Version 4.1 software (Olympus, UK). The viability of the cells was assessed at 7, 14 and 21 days using the Live/Dead Assay Kit (Invitrogen, United Kingdom) according to the manufacturer's instructions. Calcein-AM ester was used to fluorescently label viable cells (green); the nucleus of dead cells is labelled with Propidium Iodide (red). Briefly, cell culture media was removed from samples. They were washed with 1.0 mL PBS then immersed in 0.5 mL PBS staining solution containing 10 μM Calcein-AM and 1 μM Propidium Iodide and incubated at 37°C for 20 minutes in the dark. The samples (n=1) were then washed once with 1.0 mL of PBS and immediately imaged using CLSM.

Cells activity and proliferation

The Quant-iT^{TM} Picogreen® dsDNA assay kit (Invitrogen, United Kingdom) was used according to the manufacturer's instruction. The Picogreen solution was prepared as 1: 200 dilutions in 1 X Tris-EDTA (TE) buffer. Ranges of DNA dilutions (0-2 μg/mL) were used to construct a standard curve. 100 μL of cell lysate or DNA standard was placed each well of a 96 well plate, followed by 100 μL of Picogreen reagent to each well. This was placed in the dark for 5 minutes before reading the fluorescence at 485/535 nm (excitation/emission) using Synergy II BioTek plate reader.

Alkaline phosphatase (ALP) activity was obtained from a 4-Methylumbelliferyl phosphate, 4-MUP (Sigma-Aldrich, United Kingdom) reaction. Ranges of 4-Methylumbelliferone, 4-MU (Sigma-Aldrich, Switzerland) dilutions (0-2 μg/mL) were used to construct a standard curve. 50 μL of the cell lysate from each sample or standard of 4-MU and 50 μL of 4-MUP was then added into the relevant well of 96 well plate to this followed by incubation at 37°C for 90 minutes. To terminate the reaction, 100 μL of 1 X TE was added and the reading of the fluorescence was taken at 360/440 nm (excitation/emission) using Synergy II BioTek plate reader.

Cell metabolism

The levels of total protein were quantified using Bradford reagent (Sigma-Aldrich, United Kingdom). Ranges of protein standard solutions (0-2 mg/mL) were prepared by dissolving Bovine Serum Albumin, BSA (Sigma-Aldrich, United Kingdom) in distilled water. For total protein assay, 50 μL samples or standards were placed in each well of 96 well plates, followed by addition of 50 μL of Bradford reagent. Samples were incubated for 5 minutes at room temperature before reading the absorbance level at 595 nm using Synergy II BioTek plate reader.

Statistical analysis

Quantitative data were presented as means±standard deviation (SD). Data were initially tested for normality using the Kolmogorov-Smirnov test, with Dallal-Wilkinson-Lillie for corrected P value. To determine any differences between powders group at each time point, a two-way ANOVA with multiple comparisons Tukey test was performed. Statistical significance was considered for $p \leq 0.05$ (*),

$p \leq 0.01$ (**), $p \leq 0.001$ (***) and $p \leq 0.0001$ (****). For biochemical assays, tests were performed on $n=3$ in duplicate. All statistical analyses were performed using GraphPad Prism 7 software.

RESULTS

Physico-chemical characterizations

XRD analysis

Regardless of powder formulations, all powders remained stable in a single-phase diffraction pattern, typical of hydroxyapatite, HA (ICDD: 09-0432). Varying the calcination temperature from 500°C to 700°C shows no obvious difference between the diffraction patterns as shown in Fig. 1. However, the crystallographic properties showed evident effects on the lattice parameters and crystallite size of the calcined powders (Table 2). There were eight main peaks detected, i.e. at about 2θ=26° which was indexed at (002), 2θ=32-34° which represents three overlapped peaks of (211), (300) and (202), 2θ=39.8° indexed to (310), 2θ=49.4° for (222), and 2θ= 50 and 53° indexed to (213) and (004), respectively. Powders containing carbonate demonstrated a contraction in *a*-axis and expnasion in *c*-axis while carbonate-free powders (SiHA) showed expansions in both *a*- and *c*-axes at any calcination temperature. No other phase of calcium phosphate, such as calcium oxide (2θ=37.3°) was traced even at high calcination temperature of 700°C.

FTIR analysis

The full FTIR spectra scanned at 650-4000 cm^{-1} and their typical bands of the CO_3 and SiO_4 ions substituted into the apatite structure are represented in Fig. 2 for CHA, SiHA, SiCHA-1 and SiCHA-2 powders calcined at 500-700°C. For CHA and SiHA powders (Fig. 2 a and b), the typical peaks of hydroxyl groups were detected at

3570 and 1643 cm^{-1}, while only one main peak of hydroxyl was detected at 3570 cm^{-1} for SiCHA-1 and SiCHA-2 calcined powders (Fig. 2c and d) [6, 32].

All calcined powders showed the main characteristic bands of phosphate groups at about 960, 1020 and 1080 cm^{-1} as these are the most intense peaks in characterizing the hydroxyapatite crystals structure [33, 34]. The IR spectra also confirmed that there is no other secondary phase such as calcite ~712 cm^{-1}, aragonite ~713 and 700 cm^{-1} and vaterite ~745 cm^{-1} were observed for all samples [34, 35].

All CHA calcined powders regardless of the calcination temperature produced bands corresponding to the B-type CHA at about 870-875, 1410-130 and 1450-1470 cm^{-1} [12, 13, 36]. For SiCHA -1 and SiCHA-2 calcined powders, a missing band of CO_3 at 870-875 cm^{-1} was observed and only two main bands of CO_3 were found at 1410-1430 and 1450-1470 cm^{-1}. Despite of the missing band, no carbonation occurred at the hydroxyl sites (A-type CHA) which is normally detected at 877-880, 1500 and 1540-1545 cm^{-1} [13, 33, 37] in any composition of the calcined powders at 700°C.

The typical bands of Si-substituted HA (SiO_4) structure were detected at 947 and 880 cm^{-1} [26, 29] in the SiHA calcined powders at 500-700°C. Again, both SiCHA calcined powders demonstrated the absence of one of the Si-substituted HA band at about 947 cm^{-1}. A careful inspection of the IR spectra shows a small band of SiO_4 at 880-890 cm^{-1} for both SiCHA-1 and SiCHA-2 regardless the calcination temperature. Since the band of SiO_4 appears to be too small to be observed on the spectra, the results of FTIR analysis of the calcined powders was listed in Table 3 for a clear comparison between the samples.

TEM imaging

The TEM micrographs of the calcined powders at 500°C are shown in Fig. 3. The CHA powders appeared to be more spherical (20-30 nm length, 10-30 nm width) compared to pure SiHA, which have elongated rod-like particles (50-100 nm length, 15-30 nm width). At 500°C, both SiCHA-1 and SiCHA-2 powders produced particles with dimensions which fall in the range of 30-50 nm length and 15-30 nm width, perfectly matching the dimension of biological apatites [38]. The particle sizes of the calcined powders correlates well with the crystallite sizes obtained from XRD analysis, where the same trends were seen in both analyses.

CHN analysis

CHN analysis clearly demonstrated that the CO_3-substituted HA calcined powders, namely the CHA, SiCHA-1 and SiCHA-2 exhibited the loss of CO_3 as the temperature increased (Table 4). For example, even at a low calcination temperature of 500°C, there is about 21% CO_3 loss from the CHA powders; a similar trend is seen for SiCHA-1 and SiCHA-2. While, CO_3-free HA (SiHA) calcined powders showed an increment in the percentage of CO_3 with increasing temperature. However, the percentage of CO_3 present in the SiHA calcined powder is relatively low as compared to the CO_3-substituted HA powders given any calcination temperature.

Elemental analysis

The ICP-OES and XRF elemental analyses suggested that the ionic substitutions either the CO_3 and/or Si have a significant effect on the ratio of Ca/P. The ratio of Ca/P obtained for all the calcined powders are significantly higher than the stoichiometric HA which is 1.67. Higher amount of Si was detected in SiCHA-1

as compared to SiHA and SiCHA-2 at all given calcination temperatures. Regardless of the powder formulation, all Si-substituted HA powders contains <1wt% Si incorporated in the HA lattice (Table 5). It was stated that the amount of Si present *in vivo* within the mineralising osteoid regions was 0.5wt% by Carlisle (1970) [20]. Hence, the SiCHA produced in this work could be considered comparable to the mineral content found in bone *in vivo*.

In vitro biocompatibility test

Using the physico-chemical characterizations, a calcination temperature of 500°C was chosen as the optimal calcination temperature and the optimum powder compositions were CHA, SiHA, SiCHA-1 and SiCHA-2. The osteogenic effects of these optimised powders were then investigated using human bone marrow-derived mesenchymal stem cells (hMSCs).

Cell viability

CLSM images for the controls and calcined powders at 500°C after 7, 14 and 21 days in culture are presented in Fig. 4. Cells in direct contact particularly with CHA, SiHA and SiCHA-2 powders demonstrated an elongated fibroblast-like morphology consistent with the positive control at each time-point. While, SiCHA-1 revealed a lower proportion of live cells relative to SiCHA-2, SiHA and CHA powders throughout the culture. However, none of the tested powders demonstrated a toxic effect, indicated by rounded cell nucleus as observed in the negative control.

Cell proliferation and osteogenic activity

The obtained DNA concentrations suggested that all the investigated powders stimulated cell proliferation (Fig. 5 a). When comparing the powders with each other there was no significant difference between SiCHA-1, CHA and SiHA on day 7, but SiCHA-2 was significantly higher over SiCHA-1 (p=0.0021). Overall, SiCHA-2 showed the highest DNA concentrations compared to all other investigated groups (TCP and powders) on day 14 and day 21 ($p \leq 0.0001$).

ALP activity was clearly increased over time for all the tested powders (Fig. 5 b) with cells cultured on SiCHA-2 showed the highest mean ALP/DNA at either time-point (p≤0.0001). Between the single substitution powders, CHA showed significantly higher levels of mean ALP/DNA relative to SiHA as culture progressed (p≤0.0001). SiCHA-1 demonstrated similar trend to CHA, where the levels of ALP/DNA of SiCHA-1 significantly higher as compared to SiHA on day 14 (p=0.0047) and day 21 (p=0.0007).

Total protein production

The total protein production followed the behaviour of cell number indicates by the DNA concentrations where SiCHA-1 had the lowest levels mean total protein among the tested powders but still significantly higher compared to TCP on day 7 (p=0.0006) and day 14 (p≤0.0001). However, the cells in direct contact with SiCHA-1 produced lower level of total protein compared to TCP on day 21 (p≤0.0001). Overall, cells on SiCHA-2 produced the highest total protein compared to all other investigated groups (TCP and powders) on day 7, 14 and 21 (p≤0.0001).

DISCUSSION

Chemical modification of HA through ionic substitution has demonstrated benefits in accelerating bone regeneration and facilitated cell-mediated resorption of the ceramic scaffold compared with the use of stoichiometric HA [6, 8]. However, the delivering of these ionic substitutions to the targeted cells should be in controlled amounts; mimicking as is presents in the native bone, i.e. carbonate (up to 8wt%), and silicon (up to 1wt%) besides calcium and phosphate as the major components [8, 19, 39].

SiCHA with different degrees of CO_3 and Si ionic substitutions (were successfully produced in this study by chemical modification of the nanoemulsion method. Calcination treatment is a mandatory step for producing high performance scaffolds for BTE application. The main aim of calcination treatment is to ensure that the synthesis process is completed and any unreacted components incorporated during synthesis are eliminated [27, 40]. CO_3 loss in air generally starts at 550°C and is completed above 900°C, depending on treatment-time and composition [13, 41]. Therefore, the calcination temperature was limited up to 700°C for 1 hour (soaking period) in this study to retain the CO_3 content.

The physical and chemical analyses established that simultaneous substitution of CO_3 and Si ions into the HA lattice remained as pure single phase HA at 500 to 700°C. The absence of (112) Miller's plane, which usually appears on a standard HA diffraction pattern is typically attributed to the substitution of the ions into the HA structure [42]. The increased in the crystallite size of the powders with the increased of calcination temperature could be easily explained as higher calcination temperature leads to an increase in the atomic mobility, which gives rise in the grain growth resulting in a larger crystallite size.

The IR spectrum shows a clear comparison between CHA, SiHA and SiCHA after calcination. Both SiCHA calcined powders demonstrated similar characteristics with missing bands of CO_3 and Si ions at 870-875 $cm^{-1}$and 947 cm^{-1}, which is one of the typical bands of B-type CHA and Si-substituted HA, respectively. These missing bands in SiCHA powders provide evidence of the competitive substitutions between the CO_3 and Si ions into the phosphate sites.

The low calcination temperature used in this work allow the powders to remain as B-type CHA and not transforming from B-type to more complex mixture of AB-type or A-type CHA. This phase transformation normally occurs when as-synthesized powders are heat treated between 700-1200°C [32, 37, 43]. This indicated that the calcined powders produced in this study are thermally stable up to 700°C.

Surprisingly, carbonate-free substituted HA (SiHA) powders showed an increment in the percentage of CO_3 as the calcination temperature increased but was not detected in the IR spectra. This means that the CO_2 from the atmosphere was absorbed only on the surface of the powders during calcination and not incorporated in the crystal structure. The small amount of CO_3 in SiHA might also be due to the presence of acetate group that would have remained from the silicon acetate precursor [32]. In order to prevent any carbonation in the SiHA structure, the calcination of the powders could be performed in argon atmosphere instead of air [2]. At this stage of study, we concluded that 500°C was chosen as the optimum condition to produce highly controlable amounts of CO_3- and/or Si-substituted HA nanopowders which remained as single phase B-type CHA and possess similar composition to the inorganic components of bone mineral.

The surface morphologies of the optimised powders were found to be relatively differences in the particles size and shape, due to the differences in ionic

substitutions. The presence of high CO_3 concentrations in the CHA powders caused the powders to be more spherical; which is a similar observation made by Zhou et al. (2008) [27]. On the other hand, SiHA powders possess more elongated and larger particle size with about 80-100 nm in length. Both SiCHA powders produced in this study perfectly matched the dimensions of the biological apatite with particle sizes falling in the range of 30-50 nm in length and 15-30 nm in width [38]. It is important to ensure that the powders produced are at the nanoscale level in particular for BTE applications as it directly affects the mechanical and biological performances of the end products. It was shown in literature that nanoparticle apatite greatly influences variety of metabolic functions and remodelling processes [44]. For instance, *in vitro* tests of fibroblast and osteoblasts cells on the nanocrystalline octacalcium phosphate (OCP) coatings, proved that both cell types could adhered, formed a normal morphology, proliferated and remained viable, thus supporting a good biocompatibility and absence of any toxicity effects.

Despite their composition, no sign of toxicity was evident from any of the powders using a direct contact method with hMSCs. It was previously reported that the toxicity of a material is mainly caused by either the release of ions or compounds, or worn debris from the ceramic material itself [45]. In the present finding, we observed that the cells in direct contact with SiCHA-1 powders were less confluent than the other tested powders at each time-point. This is due to high ion released from SiCHA-1 powders as it contains the highest Si (0.58wt%) content among them. This abrupt ion released at early stage of culture (before 7 days) could have a negative impact on the cell viability, which caused in a slight loss of cells [8]. This is because some of the hMSCs were detached from the powders and resulted in suspended cells present in the media. Being an anchorage-dependent cells, hMSCs need a substrate to

attach and survive. When the detached cells were in suspension, they were floating and might have been discarded during media changed. Thus, less dead cells shown by the live/dead staining particularly on day 7 as compared to other tested powders. But, the population of the viable cells in direct contact with SiCHA-1 were found to remains low at every time point. However, <30% of cell death were found on all the exposed powders at 21 days. According to ISO 10993-5, a reduction of >30% viability is considered as cytotoxic. Thus, SiCHA-1 prepared in this study is considered as non-toxic, but is hindering the proliferation of hMSCs. Similar observation was reported by Landi et al. (2010) in their finding, where 0.8wt% Si in SiCHA powders caused a toxic effect on the human osteoblast cells, while SiCHA powders with lower Si content (0.55wt%) inhibited the proliferation of human osteoblast, but after 7 days of culture, powders were not considered to be toxic [8]. The higher the Si content incorporated in the HA structure, the higher the cell death. This is due to higher ion release as powders with high Si content have higher solubility [46, 47]. In this work, SiCHA-2 which contain <0.55wt% Si shows higher cell viability compared to SiCHA-1 with >0.55wt% Si. The same trend is also shown quantitatively by the DNA concentrations (Fig. 5a), which indicates the number of cell population.

After 21 days culture, SiCHA-2 shows the highest level of ALP/DNA ratio, which indicates the powder may stimulate osteogenic behaviour to greater extent than other powders. Botelho et al. (2006) found a similar behaviour up to 21 days and decreased in the ratio of ALP/COL I after 27 days treatment, which was related to the onset of mineralization [48]. However, the later trend was not observed in this study as the culture was terminated on day 21. Further work in the future, including

immunostaining, qPCR and flow cytometry would provide better indications for the osteogenic bone markers.

Carbonate-substituted HA appeared to perform better than other powders in the production of total protein after 21 days culture. This indicated that hMSCs were the most metabolically active when in contact with CHA powders. Higher CO_3 content resulted in higher metabolic activity of the particular cells/tissues [49-51]. For instance, bone, which is very active tissue, contained higher CO_3 compared to almost inert enamel [7, 8]. When comparing the SiCHA powders, SiCHA-2 shows relatively higher protein production than SiCHA-1. This is related to the cell number as represented by the amount of DNA obtained. Essentially, as the cell population increases in size so does the quantity of total protein. In addition, SiCHA-2 powders contained higher CO_3 content as compared to SiCHA-1.

CONCLUSIONS

The solubility-reactivity and biomaterial-cell interactive surfaces are two key points in determining the cell survival and response. Thus, controlled amounts of the ionic substitutions into the apatite structure are mandatory in order to promote the desired osteoblast behaviour. In this study, powders with 3.98wt% carbonate and 0.45wt% Si-substituted HA namely, SiCHA-2, shows the closest compositions to the physiological range of ionic substitutions in bone mineral, thus, make it the most favourable growth environment for hMSCs up to 21 days culture *in vitro*. These powders were associated with the most rapid proliferation of cells showed the strongest potential for osteogenic activity (ALP/DNA ratio). hMSCs also produced more proteinaceous material and were most metabolically active in direct contact with SiCHA-2 as compared to SiCHA-1. It can be concluded at this point that, among the

tested powders, SiCHA-2 was the best powder formulation and that it was suitable for the next phase in the development of a novel 3D SiCHA scaffold for BTE.

ACKNOWLEDGEMENTS

The authors would like to thanks Arthritis Research United Kingdom-Tissue Engineering Centre (ARUK-TEC) and the Ministry of Higher Education Malaysia (MOHE) for supporting this work.

REFERENCES

[1] Tripathi G, Basu B. A porous hydroxyapatite scaffold for bone tissue engineering: Physico-mechanical and biological evaluation. Ceram. Int. 2012; 38(1): 341-349.

[2] David M, Guénaële B, Aline L, Maria Z, Luc M, Stéphanie S, Nicolas D, Didier B-A, Jérôme C. Physico-chemical characterization and in vitro biological evaluation of pure SiHA for bone tissue engineering application. Key Eng. Mat. 2013; 529-530: 351–356.

[3] Cox S, Thornby JA, Gibbons GJ, Williams MA, Mallick KK. 3D printing porous hydroxyapatite scaffolds intended for use in bone tissue engineering applications. Mat. Sci. Eng. C 2015; 47: 237-247.

[4] Pon-On W, Suntornsaratoon P, Charoenphandhu N, Thongbunchoo J, Krishnamra N, Tang IM. Hydroxyapatite from fish scale for potential use as bone scaffold or regenerative material. Mat. Sci. Eng. C 2016; 62: 183-189.

[5] Magnaudeix A, Usseglio J, Lasgorceix M, Lalloue F, Damia C, Brie J, Pascaud-Mathieu P, Champion E. Quantitative analysis of vascular colonization and angio-conduction in porous silicon-substituted hydroxyapatite with various pore shapes in a chick chorioallantoic membrane (CAM) model. Acta Biomateriallia 2016; 38: 179-189.

[6] Sprio S, Tampieri A, Landi E, Sandri M, Martorana S, Celotti G, Logroscino G. Physico-chemical properties and solubility behaviour of multi-substituted hydroxyapatite powders containing silicon. Mater. Sci. Eng. C 2008; 28(1): 179–187.

[7] Boanini E, Gazzano M, Bigi A. Ionic substitutions in calcium phosphates synthesized at low temperature. Acta biomaterialia 2010; 6(6): 1882–1894.

[8] Landi E, Jacopo U, Sprio S, Tampieri A, Guizzzardi S. Human osteoblast behavior on as-synthesized SiO(4) and B-CO(3) co-substituted apatite. J. Biomed. Mater. Res.-A 2010; 94(1): 59–70.

[9] Lala S, Ghosh M, Das PK, Das D, Kar T, Pradhan SK. Magnesium substitution in carbonated hydroxyapatite: Structural and microstructural characterization by Rietveld's refinement. Mater. Chem. Phy. 2016; 170: 319-329.

[10] Baba Ismail YM & Mohd Noor AF. Effect of a novel approach of sintering on physical properties of carbonated hydroxyapatite. J. Mater. Sci. Eng. B 2011; 1(2): 157–163.

[11] Kee CC, Ismail H, Mohd Noor AF. Effect of synthesis technique and carbonate content on the crystallinity and morphology of carbonated hydroxyapatite. J. Mater. Sci. Tech. 2013; 29 (8): 761-764.

[12] Xue C, Chen Y, Huang Y, Zhu P. Hydrothermal synthesis and biocompatibility study of highly crystalline carbonated hydroxyapatite nanorods. Nanoscale Res. Lett. 2015; 10: 316-322.

[13] Liu Q, Matinlinna JP, Chen Z, Ning C, Ni G, Pan H, Darvell BW. Effect of thermal treatment on carbonated hydroxyapatite: Morphology, composition, crystal characteristics and solubility. Ceram. Int. 2015; 41(5): 6149-6157.

[14] Landi E, Celotti G, Logroscino G, Tampieri A. Carbonated hydroxyapatite as bone substitute. J. Eur. Ceram. Soc. 2003; 23(15): 2931–2937.

[15] Boyer A, Marchat D, Bernache-Assollant D. Synthesis and characterization of Cx-Siy-HA for bone tissue engineering application. Key Eng. Mat. 2013; 529-530: 100-104.

[16] Murugan R & Ramakrishna S. Production of ultra-fine bioresorbable carbonated hydroxyapatite. Acta biomaterilia 2006; 2(2): 201–206.

[17] Shepherd JH, Shepherd DV, Best SM. Substituted hydroxyapatites for bone repair. J. Mater Sci. – Mater. Med. 2012; 23(10): 2335–2347.

[18] Porter A, Patel N, Brooks R, Best S, Rushton N, Bonfield W. Effect of carbonate substitution on the ultrastructural charac- teristics of hydroxyapatite implants. J. Mater. Sci. Med. 2005; 16: 899.

[19] Hing KA, Revell PA, Smith N, Buckland T. Effect of silicon level on rate, quality and progression of bone healing within silicate-substituted porous hydroxyapatite scaffolds. Biomaterials 2006; 27: 5014–5026.

[20] Carlisle EM. Silicon: A possible factor in bone calcification. Science 1970; 167: 279–280.

[21] Schwarz K & Milne DB. Growth-promoting effects of silicon in rats. Nature 1972, 239: 333–334.

[22] Carlisle EM. Silicon: an essential element for the chick. Science 1972;178:619–621.

[23] Reffitt DM, Ogston N, Jugdaohsingh R, Cheung HFJ, Evans BAJ, Thompson RPH, Powell JJ, Hampson GN. Orthosilicic acid stimulates collagen type I synthesis and osteoblastic differentiation in human osteoblast-like cells in vitro. Bone 2003; 32(2): 127-135.

[24] Jugdaohsingh R. Silicon and Bone Health. J. Nutr. Health Aging 2007; 11(2): 99-110.

[25] Pietak AM, Reid JW, Stott MJ, Sayer M. Silicon substitution in the calcium phosphate bioceramics. Biomaterials 2007; 28(28): 4023–4032.

[26] Douard N, Leclerc L, Sarry G, Bin V, Marchat D, Forest V, Pourchez J. Impact of the chemical composition of poly-substituted hydroxyapatite particles on the in vitro pro-inflammatory response of macrophages. Biomed. Microdevices 2016; 18:27.

[27] Zhou WY, Wang M, Cheung WL, Guo BC, Jia DM. Synthesis of carbonated hydroxyapatite nanospheres through nanoemulsion. J. Mater. Sci.- Mater Med. 2008; 19(1): 103–110.

[28] Bianco A, Cacciotti I, Lombardi M, Montanaro L. Si-substituted hydroxyapatite nanopowders: synthesis, thermal stability and sinterability. Mater. Res. Bull. 2009; 44: 345–354.

[29] Marchat D, Zymelka M, Coelho C, Gremillard L, Joly-pottuz L, Babonneau F, Esnouf C, Chevalier J, Bernache-assolant D. Accurate characterization of pure silicon-substituted hydroxyapatite powders synthesized by a new precipitation route. Acta Biomaterialia 2013; 9: 6992-7004.

[30] Nakamura M, Hentunen T, Salonen J, Nagai A, Yamashita K. Characterization of bone mineral-resembling biomaterials for optimizing human osteoclast differentiation and resorption. J. Biomed. Mater. Res.-A 2013; 101A(11): 3141-3151.

[31] Krajewski A, Mazzocchi M, Buldini PL. Ravaglioli A, Tinti A, Taddei P, Fagnano C. Synthesis of carbonated hydroxyapatites: efficiency of the substitution and critical evaluation of analytical methods. J. Mol. Struct. 2005; 744-747: 221-28.

[32] Gibson IR & Bonfield W. Novel synthesis and characterization of an AB-type carbonate-substituted hydroxyapatite. J. Biomed. Mater. Res. 2002; 59(4): 697–708.

[33] Koutsopoulos S. Synthesis and characterization of hydroxyapatite crystals: A review study on the analytical methods. J. Biomed. Mater. Res. 2002; 62(4): 600-612.

[34] Landi E, Tampieri A, Celotti G, Vichi L, Sandri M. Influence of synthesis and sintering parameters on the characteristics of carbonate apatite. Biomaterials 2004; 25: 1763-1770.

[35] Ślósarczyk A, Paszkiewicz Z, Paluszkiewicz C. FTIR and XRD evaluation of carbonated hydroxyapatite powders synthesized by wet methods. J. Mol. Struct. 2005; 744-747: 657–661.

[36] Bang LT, Long BD, Othman R. Carbonate hydroxyapatite and silicon-substituted carbonate hydroxyapatite: synthesis, mechanical properties, and solubility evaluations. Scientific World J. 2014: 969876.

[37] Lafon JP, Champion E, Bernache-Assollant D. Processing of AB-type carbonated hydroxyapatite $Ca_{10-x}(PO_4)_{6-x}(CO_3)x(OH)_{2-x-2y}(CO_3)_y$ ceramics with controlled composition. J. Eur. Ceram. Soc. 2008; 28(1): 139–147.

[38] Wang YJ, Chen JD, Wei K, Zhang SH, Wang XD. Surfactants-assisted synthesis of hydroxyapatite crystals. Mater. Lett. 2006; 60: 3227-3231.

[39] Gibson IR, Best SM, Bonfield W. Effect of silicon substitution on the sintering and microstructure of hydroxyapatite. J. Am. Ceram. Soc. 2002; 85: 2771–2777.

[40] Scalera F, Gervaso F, Sanosh KP, Sannino A, Licciulli A. Influence of calcination temperature on morphological and mechanical properties of highly porous hydroxyapatite scaffolds. Ceram. Int. 2013; 39(5): 4839-4846.

[41] Ivanova TI, Kamenetskaya F, Kol'tsov AB, Ugolkov VL. Crystal Structure of Calcium-Deficient Carbonated Hydroxyapatite. Thermal Decomposition. J. Solid State Chem. 2001; 160(2): 340–349.

[42] He QJ, Huang ZL, Cheng XK, Yu J. Thermal stability of porous A-type carbonated hydroxyapatite spheres. Mater. Lett. 2007; 62: 539-542.

[43] LeGeros RZ, Trautz, OR, Klein E, LeGeros JP. Two types of carbonate substitution in the apatite structure. Experientia 1969; 25(1955): 5–7.

[44] Dorozhkin SV. Calcium orthophosphates in nature, biology and medicine. Materials 2009; 2: 399-498.

[45] Li J, Liu Y, Hermansson L, Söremark R. Evaluation of Biocompatibility of Various Ceramic Powders with Human Fribroblasts in vivo. Clin. Mater. 1993; 12: 197-201.

[46] Lin W, Huang YW, Zhou XD, Ma Y. In vitro toxicity of silica nanoparticles in human lung cancer cells. Toxicol. Appl. Pharm. 2006; 217: 252–259.

[47] Ni S, Chang J, Chou L, Zhai W. Comparison of osteoblast- like cell responses to calcium silicate and tricalcium phos- phate ceramics in vitro. J. Biomed. Mater. Res.-B 2007; 80:174–183.

[48] Botelho CM, Brooks RA, Spence G, McFarlane I, Lopes MA, Best SM, Santos JD, Rushton N, Bonfield W. Differentiation of mononuclear precursors into osteoclasts on the surface of Si-substituted hydroxyapatite. J. Biomed. Mater. Res.-A 2006; 78A: 709–720.

[49] Gibson IR, Best SM, Bonfield W. Chemical characterization of silicon-substituted hydroxyapatite. J. Biomed. Mater. Res. 1999; 44: 422-428.

[50] Nakamura M, Hiratai R, Hentunen T, Salonen J, Yamashita K. Hydroxyapatite with high carbonate substitutions promotes osteoclast resorption through osteocyte-like cells. Biomater. Sci. Eng. 2015; 259-267.

[51] Rupani A, Hidalgo-Bastida LA, Rutten F, Dent A, Turner I, Cartmell S. Osteoblast activity on carbonated hydroxyapatite. J. Biomed. Mater. Res.-A 2012; 4: 1089-1096.

FIGURE TITLES AND LEGENDS

Figure 1.

XRD analysis of the calcined powders at 500-700°C; (a) CHA; (b) SiHA; (c) SiCHA-1; (d) SiCHA-2, demonstrating single phase of HA without the formation of secondary phase. Regardless of the powders composition, no obivious differences were observed between the diffraction patterns at any given calcination temperature.

Figure 2.

FTIR spectra of (a) CHA, (b) SiHA, (c) SiCHA-1 and (d) SiCHA-2 calcined powders at 500-700°C and their typical bands of the carbonate and silicon ions substituted into the apatite structure, respectively. Regardless of the calcination temperatures, three major bands of CO_3 were observed for the CHA powders, whilst only two vibration bands detected for both SiCHA powders. CO_3-free powders (SiHA) exhited no CO_3 bands besides the two typical Si-substituted vibration bands. At any given calcination temperature, SiCHA-1 and SiCHA-2 shows a missing band of SiO_4, indicating the evidence of the competitive substitutions between CO_3 and/or Si into the phosphate sites.

Figure 3.

TEM images of the optimum calcined powders calcined at 500°C; (a) CHA; (b) SiHA; (c) SiCHA-1; (d) SiCHA-2. The particle sizes of the calcined powders correlates well with the crystallite sizes obtained from XRD analysis, where the same trends were seen in both analyses. Scale bar = 100 nm.

Figure 4.

CLSM images of the controls and optimum calcined powders of CHA, SiHA, SiCHA-1 and SiCHA-2 cultured in osteogenic media for 21 days. Green indicates viable cells and red indicates dead cells. Scale bar = 200 μm. ** PVE CTL= Positive control (hMSCs cultured in osteogenic media act as tissue culture plastic) and NVE CTL= Negative Control (hMSCs cultured in 0.1% Triton-X in high glucose expansion media). The population of viable cells in direct contact with SiCHA-1 was lower compared the other tested powders, but no toxicity effect occurred throughout the culture period.

Figure 5.

Effect of CHA, SiHA, SiCHA-1 and SiCHA-2 as-calcined powders on (a) cell proliferation indicated by the amount of DNA, (b) the ALP activity per unit cell (ALP/DNA) and (c) the levels of total protein production. Control represents the tissue culture plastic in osteogenic media (positive control). Values represent the mean±SD of three samples in duplicate. (*$p \leq 0.05$, **$p \leq 0.01$, ***$p \leq 0.001$, ****$p \leq 0.0001$). Cells in direct contact with SiCHA-2 demonstrtaed the highest DNA concentrations and total protein production than the other tested powders and controls. The lower Si content in SiCHA-2 showed the highest ALP/DNA ratio after 21 days culture with hMSCs, indicating that the powder may stimulate osteogenic behaviour to a greater extent than other powders.

TABLE TITLES AND LEGENDS

Table 1.

Different formulations of the prepared powders.

Note: Provided no carbonation in A site occurred.

Table 2.

Lattice parameters and crystallite sizes of CHA, SiHA, SiCHA-1 and SiCHA-2 powders at 500-700°C. Increasing the calcination temperature from 500 to 700°C altered the lattice parameters and increased the crystallite sizes of the calcined powders.

Table 3.

Results of FTIR analysis of the calcined powders at 500-700°C. Of the four different compositions investigates, SiCHA-1 and SiCHA-2 showed missing bands for CO_3 and Si using FTIR analysis.

Table 4.

CHN analysis of the calcined powders at 500-700°C. Powders containing CO_3 showed CO_3 loss as the calcination temperature increased. While, CO_3-free powders demonstrated an increment in CO_3 wt%, indicating the adsorption of CO_2 from the atmosphere during calcination.

Table 5.

Elemental analyses of the calcined powders at 500-700°C. The ratio of Ca/P obtained for all the tested powders are relatively higher than the stoichiometric HA (1.67), suggesting that the ionic substitutions either the CO_3 and/or Si have a significant effect on Ca/P ratio.

Figure 1

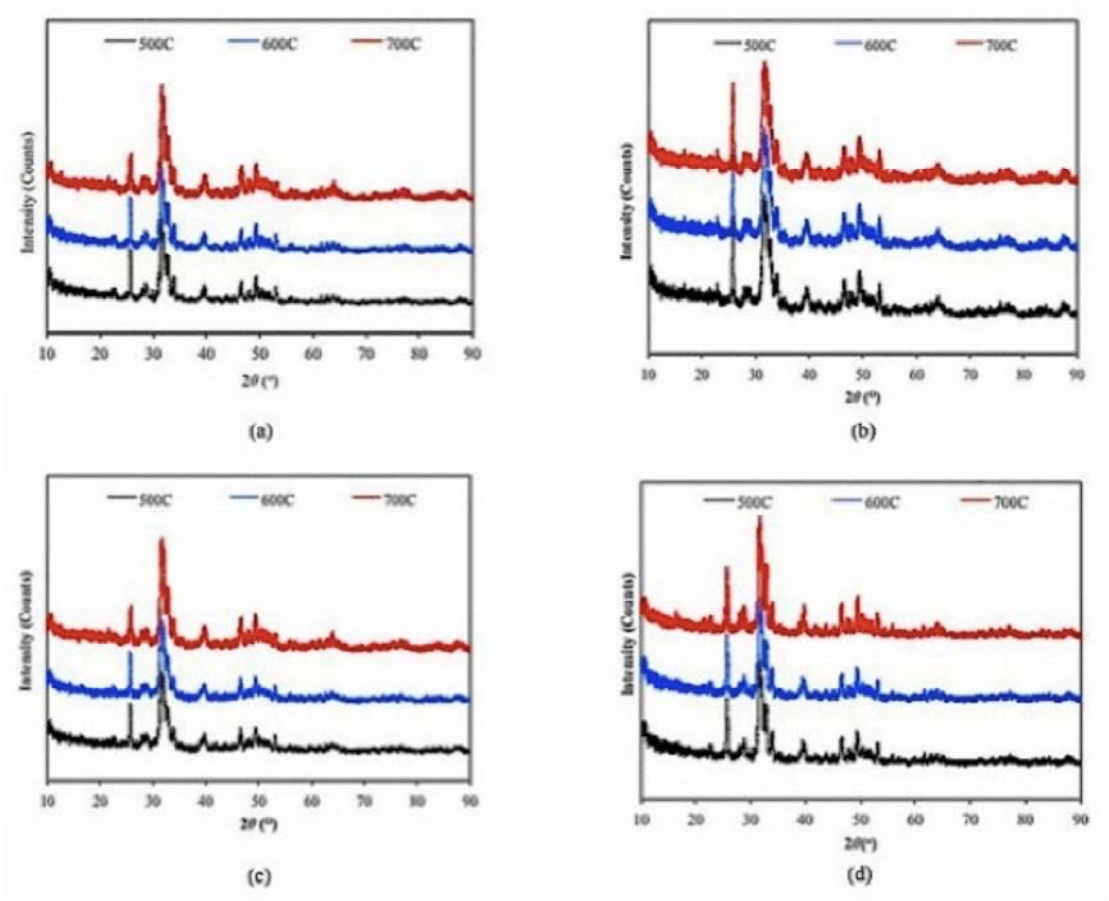

Figure 2

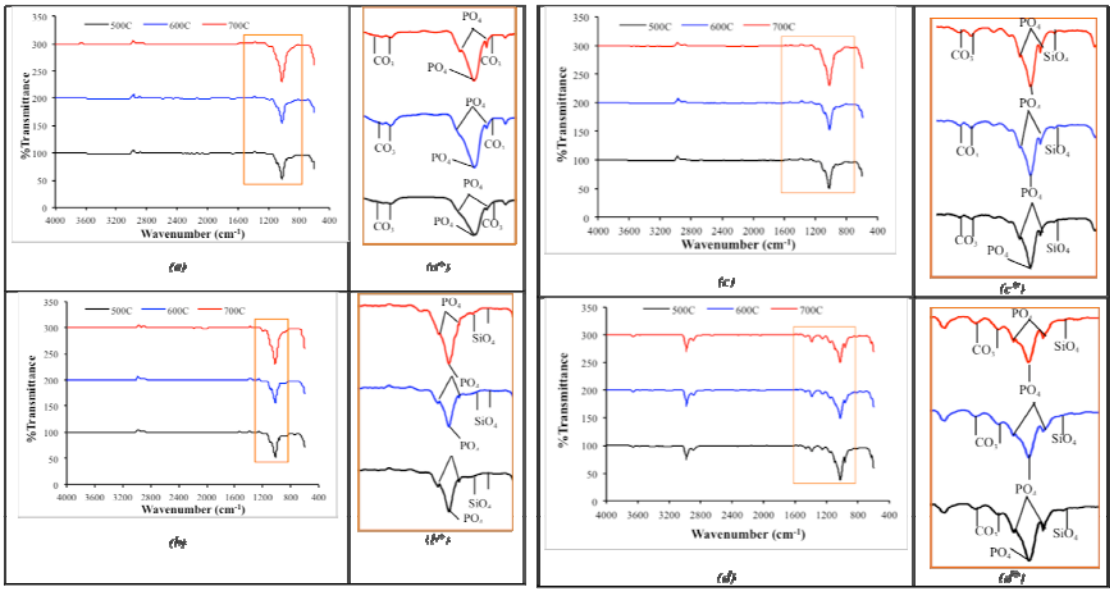

Figure 3

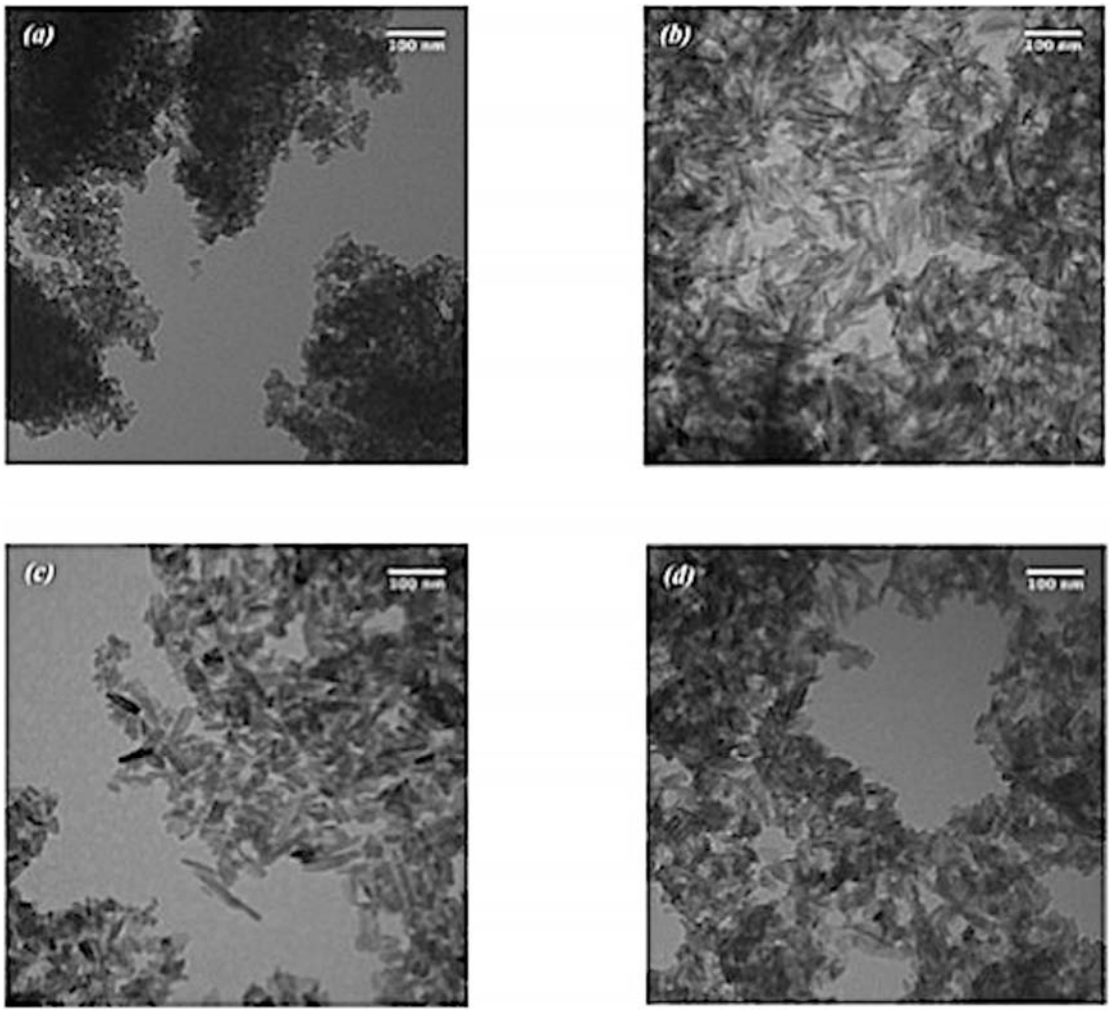

Figure 4

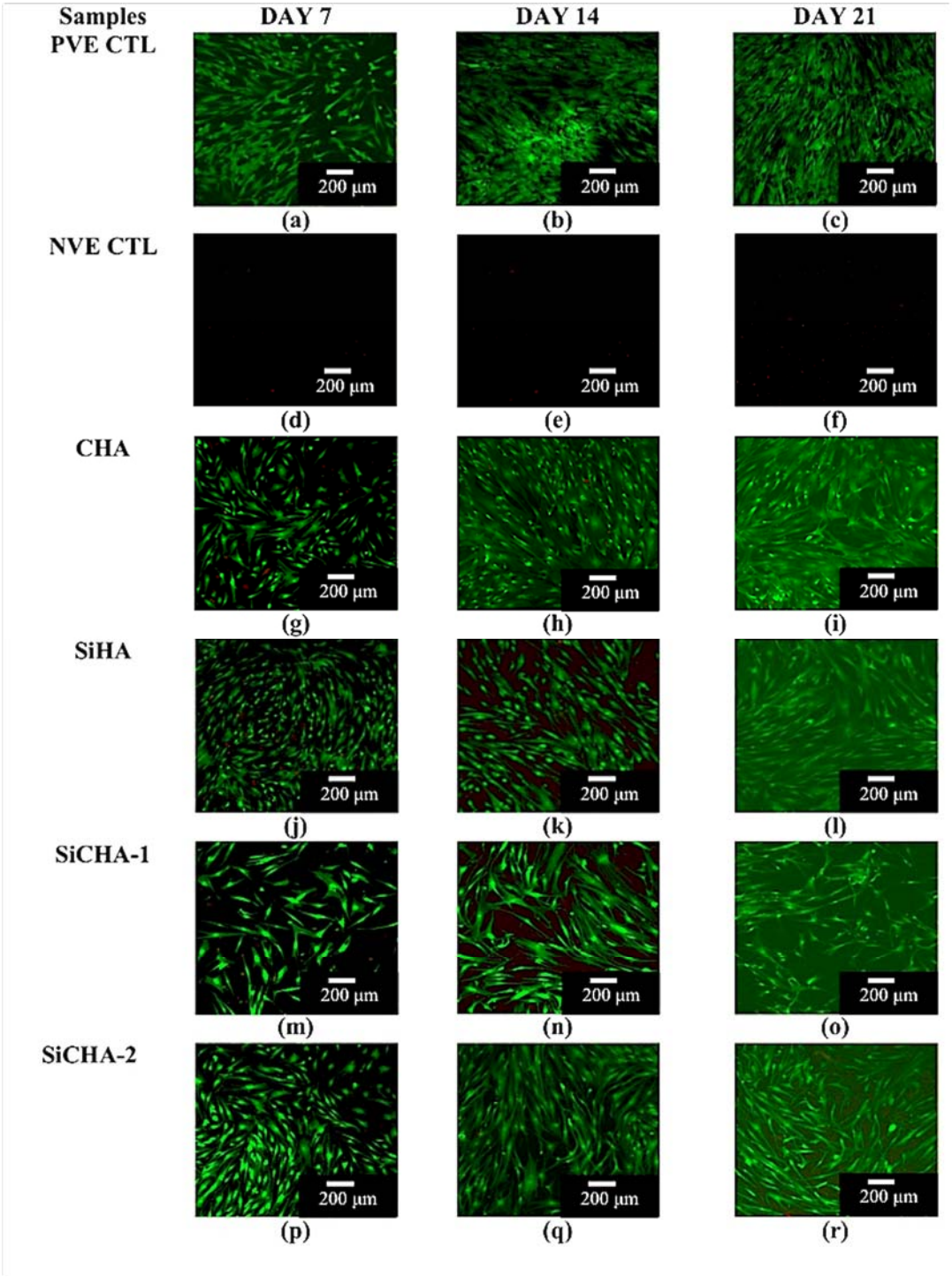
Samples
DAY 7
DAY 14
DAY 21
PVE CTL
NVE CTL
CHA
SiHA
SiCHA-1
SiCHA-2
200 µm
(a)
(b)
(c)
(d)
(e)
(f)
(g)
(h)
(i)
(j)
(k)
(l)
(m)
(n)
(o)
(p)
(q)
(r)

Figure 5

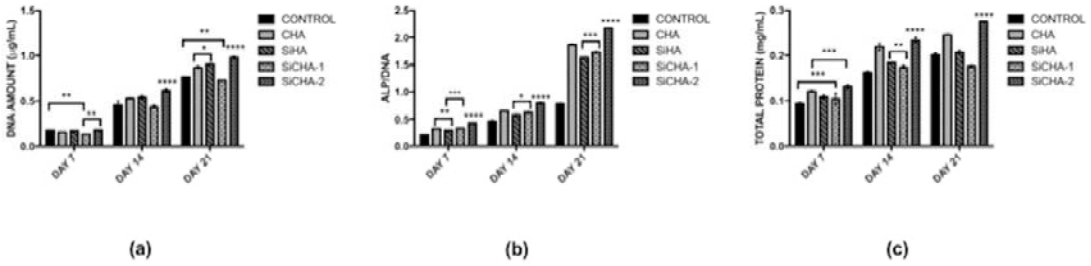

TABLES

Table 1. Different formulations of the prepared powders.

Sample codes	CO_3 (*x*)	Si (*y*)	Powders formulation
CHA	2.0	-	$Ca_9(PO_4)_4(CO_3)_2(OH)_2$
SiHA	-	0.3	$Ca_{10}(PO_4)_{5.7}(SiO_4)_{0.3}(OH)_{1.7}$
SiCHA-1	2.0	0.5	$Ca_9(PO_4)_{3.5}(CO_3)_2(SiO_4)_{0.5}(OH)_{1.5}$
SiCHA-2	2.0	0.3	$Ca_9(PO_4)_{3.7}(CO_3)_2(SiO_4)_{0.3}(OH)_{1.7}$

Note: Provided no carbonation in A site occurred.

Table 2. Lattice parameters and crystallite sizes of CHA, SiHA, SiCHA-1 and SiCHA-2 powders at 500-700°C.

Samples	Calcination temperature (°C)	Lattice parameters (Å)		Crystallite size (nm)
		***a* ± 0.003**	***c* ± 0.003**	
CHA	500	9.389	6.918	10.02
	600	9.367	6.920	17.83
	700	9.352	6.923	20.76
SiHA	500	9.452	6.921	17.21
	600	9.455	6.923	21.02
	700	9.459	6.928	28.89
SiCHA-1	500	9.399	6.901	12.86
	600	9.391	6.912	19.87
	700	9.387	6.918	23.73
SiCHA-2	500	9.378	6.898	12.09
	600	9.372	6.893	18.92
	700	9.369	6.899	21.07

Increasing the calcination temperature from 500 to 700°C altered the lattice parameters and increased the crystallite sizes of the calcined powders.

Table 3. Results of FTIR analysis of the calcined powders at 500-700°C.

Samples	T(°C)	OH	PO_4	CO_3	Si
CHA	*500*	*3573.0, 1649.7*	*962.9, 1024.4, 1083.3*	*873.7, 1414.8, 1458.8*	-
	600	*3573.3, 1643.0*	*962.5, 1020.0, 1080.0*	*873.1, 1414.8, 1454.3*	-
	700	*3573.5, 1638.2*	*962.3, 1019.9, 1081.2*	*872.7, 1417.1, 1459. 9*	-
SiHA	*500*	*3562.5, 1651.1*	*963.2, 1024.9, 1086.4*	-	*947.4, 885.7*
	600	*3569.7, 1635.8*	*962.5, 1024.7, 1089.7*	-	*946.9, 883.5*
	700	*3570.9, 1633.5*	*962.4, 1024.1, 1090.1*	-	*947.2, 884.2*
SiCHA-1	*500*	*3572.5*	*962.7, 1027.7, 1088.0*	*1418.2, 1461.9*	*883.1*
	600	*3570.8*	*962.2, 1022.9, 1087.9*	*1418.6, 1461.8*	*885.3*
	700	*3569.9*	*962.5, 1023.5, 1089.0*	*1413.6, 1461.9*	*887.7*
SiCHA-2	*500*	*3572.5*	*962.7, 1027.7, 1088.0*	*1418.2, 1461.9*	*883.5*
	600	*3578.7*	*962.2, 1022.9, 1080.0*	*1412.8, 1461.8*	*886.3*
	700	*3579.6*	*962.5, 1023.5, 1089.0*	*1418.2, 1461.3*	*884.9*

Of the four different compositions investigates, SiCHA-1 and SiCHA-2 showed missing bands for CO_3 and Si using FTIR analysis.

Table 4. CHN analysis of the calcined powders at 500-700°C.

Samples	*T(°C)*	*%C (wt%)*	*%CO_3 (wt%)*	*%CO_3 changes after calcination (wt%)*
CHA	*500*	*1.08*	*5.80*	*-21.63*
	600	*0.99*	*4.95*	*-33.11*
	700	*0.57*	*4.15*	*-43.92*
SiHA	*500*	*0.01*	*0.05*	*+125.00*
	600	*0.02*	*0.08*	*+200.00*
	700	*0.02*	*0.12*	*+300.00*
SiCHA-1	*500*	*0.48*	*2.90*	*-24.68*
	600	*0.42*	*2.25*	*-41.56*
	700	*0.36*	*1.90*	*-50.65*
SiCHA-2	*500*	*0.79*	*3.98*	*-23.50*
	600	*0.50*	*3.25*	*-37.50*
	700	*0.38*	*2.98*	*-42.69*

Powders containing CO_3 showed CO_3 loss as the calcination temperature increased. While, CO_3-free powders demonstrated an increment in CO_3 wt%, indicating the adsorption of CO_2 from the atmosphere during calcination

Table 5. Elemental analyses of the calcined powders at 500-700°C.

Samples	*T(°C)*	*Ca/P Measured value (XRF)*	*Si (wt%) Measured value (ICP-OES)*
CHA	*500*	*1.76*	*-*
	600	*1.77*	*-*
	700	*1.79*	*-*
SiHA	*500*	*1.71*	*0.49*
	600	*1.72*	*0.46*
	700	*1.74*	*0.41*
SiCHA-1	*500*	*1.89*	*0.58*
	600	*1.91*	*0.47*
	700	*1.95*	*0.43*
SiCHA-2	*500*	*1.86*	*0.45*
	600	*1.89*	*0.42*
	700	*1.92*	*0.40*

The ratio of Ca/P obtained for all the tested powders are relatively higher than the stoichiometric HA (1.67), suggesting that the ionic substitutions either the CO_3 and/or Si have a significant effect on Ca/P ratio.